Automating Treatment Planning in Radiation Therapy

Lekan Ogunmolu

Perelman School of Medicine

University of Pennsylvania, Philadelphia, PA

February 04, 2021

Collaborators/Advisors/Colleagues

Steve Jiang, UTSW

Nick Gans, UTARI

Xuejun Gu, UTSW

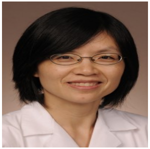

Dan Nguyen, UTSW

Rod Wiersma, Penn

Tyler Summers, UTD

Yonas Tadesse, UTD

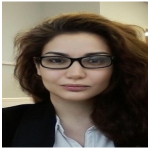

Azar S.B, UTSW

Funding Sources

NIH NATIONAL CANCER INSTITUTE

CANCER PREVENTION & RESEARCH INSTITUTE OF TEXAS

Talk Outline

- Patient Head Motion Correction in External Beam Radiation Therapy
  - Magnetic Resonance Imaging and Linear Accelerator Systems (MRI-LINACs)
  - Intensity-Modulated RT (IMRT): Earlier PhD Work
- Beam Orientation Optimization (BOO)
  - Monte Carlo Tree Search and Neuro-Dynamic Programming for BOO
  - Column Generation as Pretraining for MCTS for BOO
- Robustness Margins and Robust Deep Policies for Nonlinear Control

Research Significance

2020 → 1.8 million U.S. cancer cases [1] → > 600,000 deaths → 4.2% overall healthcare spending

Cancer Treatment

- Chemotherapy/Radiosurgery.
- Radiation Therapy (RT).

RT Signif.

- Approx. 40% of all curative cancer treatment modality are performed with RT [Baskar et al].
- Cost-effective -- accounting for only 5% of the total cost of cancer care [Ringborg et al.].

Imaging

- CT images in RT = Low soft tissues contrast ⇒ OARs toxicity during treatment planning.
- MRI of brain, and head and neck (H&N) cancers provides exceptional soft tissues contrast and allows greater delineation of cancerous from non-cancerous tissues.

IMRT Treatment Planning (Beam Delivery)

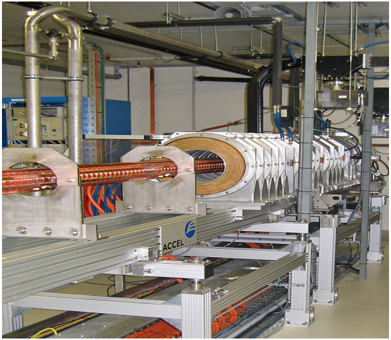

The Australian Synchrotron.

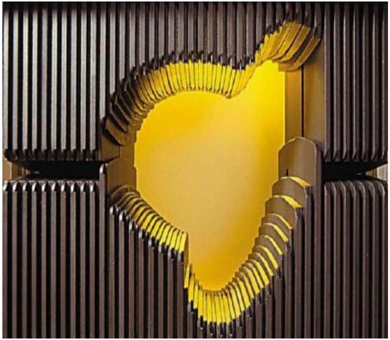

Multi-leaf collimator (Varian)

Radiation Delivery Couch and Gantry

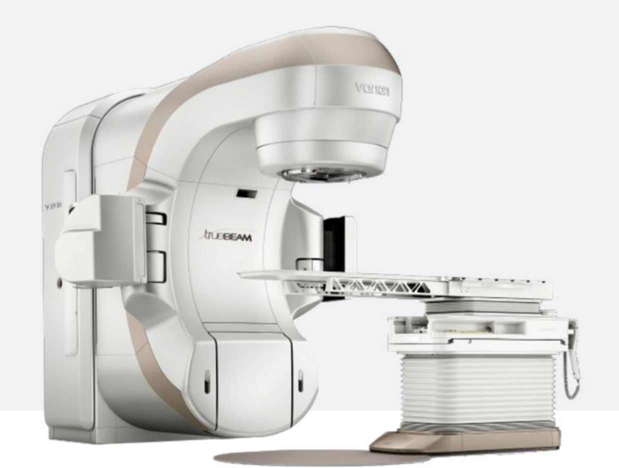

Varian's TrueBeam Radiotherapy System.

Head Stabilization in Radiation Therapy (RT)

- Head Stabilization in Cancer Radiation Therapy
  - Intensity-Modulated RT (IMRT): Earlier PhD Work

Simulation Testbed

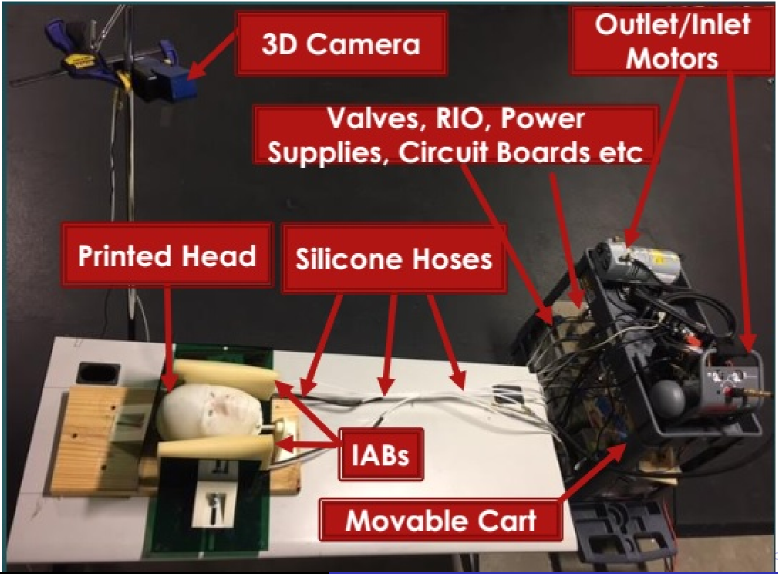

Control Design Goals

- Stabilize z, pitch, and roll states, *i.e.*

$$\boldsymbol{x} = \begin{pmatrix} z \\ \theta \\ \phi \end{pmatrix}$$

- By solving an adaptive state feedback controller, optimal regulation, and minimize parametric uncertainties

Control Design Goals

- Provide closed loop tracking given a desired trajectory, **r**
- Robustify system to (non-)parametric uncertainties

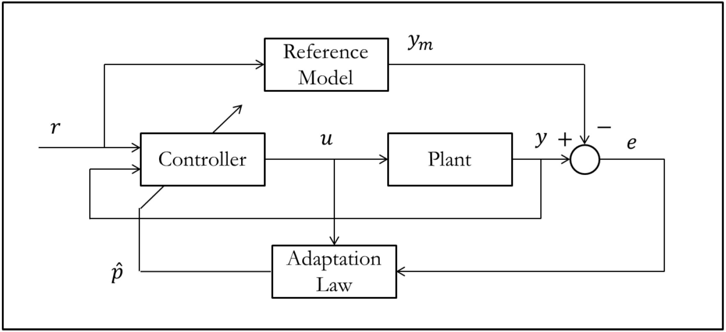

Indirect MRAC system. (Source mdpi.com)

Model Reference Adaptive Control

- Model head and bladder dynamics as
  - $\dot{\boldsymbol{x}} = \mathbf{A}\boldsymbol{x} + \mathbf{B}\boldsymbol{\Lambda}\left(\mathbf{u} - f(\boldsymbol{x}, \mathbf{u})\right) + \mathbf{w}(k)$
- Approximate $f(\boldsymbol{x}, \mathbf{u})$ by a neural network with continuous memory states
- Derive adaptive adjustment mechanism from Lyapunov analysis for Adaptive Control Parks (1966)
- $\mathbf{u} = \underbrace{\hat{\mathbf{K}}_x^{\mathbf{T}}\boldsymbol{x}}_{\text{state feedback}} + \underbrace{\hat{\mathbf{K}}_r^{\mathbf{T}}\mathbf{r}}_{\text{optimal regulator}} + \underbrace{\hat{f}(\boldsymbol{x}, \mathbf{u})}_{\text{approximator}}$

Neural Network Architecture

Neural Net Architecture

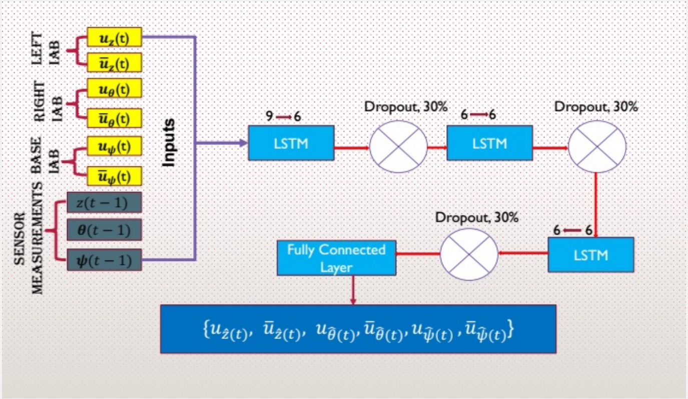

Lyapunov Redesign: Theorem

- For correct adaptive gains, $\hat{\mathbf{K}}_x$ and $\hat{\mathbf{K}}_r$, $\mathbf{e}(k)$ is ***uniformly ultimately bounded***, and the state $\boldsymbol{x}$ converges to a neighborhood of $\mathbf{r}$.
- Choose a $\mathbf{V}$ in terms of $\mathbf{e}$; $\tilde{\mathbf{K}}_x^T$, $\tilde{\mathbf{K}}_r^T$; and parameter error $\varepsilon_f(\boldsymbol{x}(k))$ space

$$\mathbf{V}(\mathbf{e}, \tilde{\mathbf{K}}_x, \tilde{\mathbf{K}}_r^T) = \mathbf{e}^T\mathbf{P}\mathbf{e} + \mathbf{tr}(\tilde{\mathbf{K}}_x^T \boldsymbol{\Gamma}_x^{-1} \tilde{\mathbf{K}}_x^T |\boldsymbol{\Lambda}|) + \mathbf{tr}(\tilde{\mathbf{K}}_r^T \Gamma_r^{-1} \tilde{\mathbf{K}}_r |\boldsymbol{\Lambda}|)$$

Stability Results: Ogunmolu et al. (2017)

$$\begin{aligned}\dot{\mathbf{V}}(\cdot) &= -\mathbf{e}^T\mathbf{Q}\mathbf{e} - 2\mathbf{e}^T\mathbf{P}\mathbf{B}\boldsymbol{\Lambda}\varepsilon_f \\ &\leq -\lambda_{low}\|\mathbf{e}\|^2 + 2\|\mathbf{e}\|\|\mathbf{P}\mathbf{B}\|\lambda_{high}(\boldsymbol{\Lambda})\varepsilon_{max}\end{aligned}$$

- $\{\lambda_{low}, \lambda_{high}\} \equiv$ min/max eigenvalues of Q and $\boldsymbol{\Lambda}$.
- $\dot{\mathbf{V}}(\cdot)$ is thus negative definite outside the compact set: $\chi = \left(\mathbf{e} : \|\mathbf{e}\| \leq \frac{2\|\mathbf{P}\mathbf{B}\|\lambda_{high}(\boldsymbol{\Lambda})\varepsilon_{max}(\mathbf{y})}{\lambda_{low}(\mathbf{Q})}\right)$
    - *i.e.* **e** is **uniformly ultimately bounded**, or $\mathbf{y}(t) \to 0$ as $t \to \infty$.

Results: Z and Pitch Motions

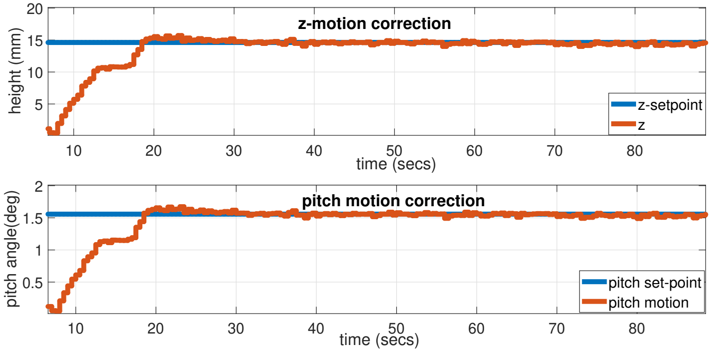

Goal command: $(z, \theta, \phi) = (14mm, 1.6^\circ, 45^\circ)^T$.

Results: Roll Motion

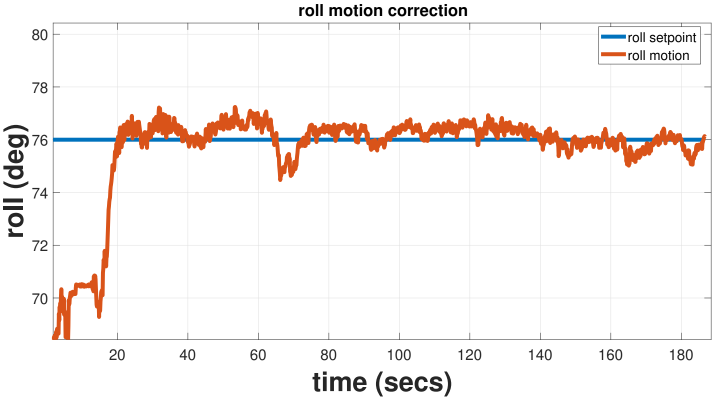

Head roll tracking.

Conclusions

- Non-invasive soft robot for head motion compensation ✓
- Photons-transparent as opposed to rigid/electro-mechanical devices/robots ✓
- Adaptible under MRI coils for newer MRI-LINACs ✓

Head Stabilization in RT

- Head Stabilization in Cancer Radiation Therapy
  - Magnetic Resonance Imaging-Linear Accelerator Systems (MRI-LINACs)

Robotic Radiosurgery

- Current Collaborators: Rodney Wiersma & Xinmin Liu (UChicago → UPenn)
- Past Collaborators: Steve Jiang, Xuejun Gu, (UT Southwestern); Nick Gans (UT Dallas, UT Arlington)

Correcting Head Motion: RT and MRI-LINACs

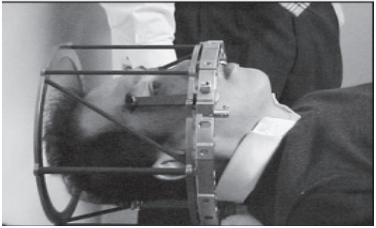

(a) The BRW SRS Frame [Chelvarajah et al. (2004)]

(b) Thermoplastic masks

(c) Frame With MRI Coils (PSOM)

4-D Motion Correction Stage

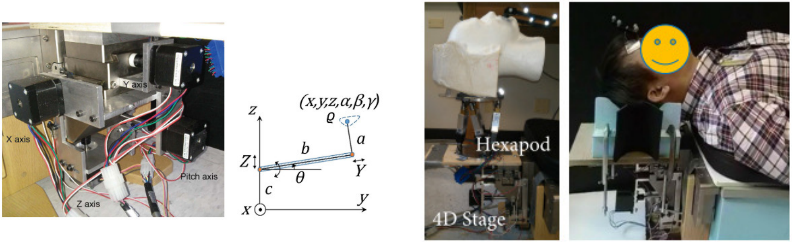

Liu et al. (2015)

4-DOF Motion Controller Block Diagram

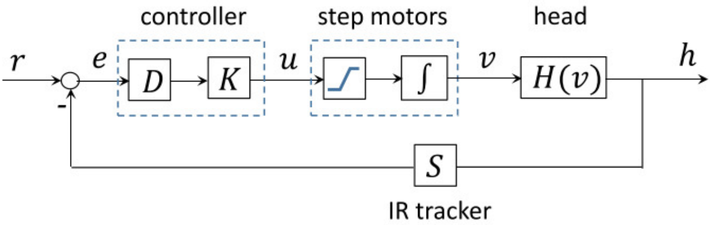

Liu et al. (2015)

Phantom Feedback Motion Correction Results

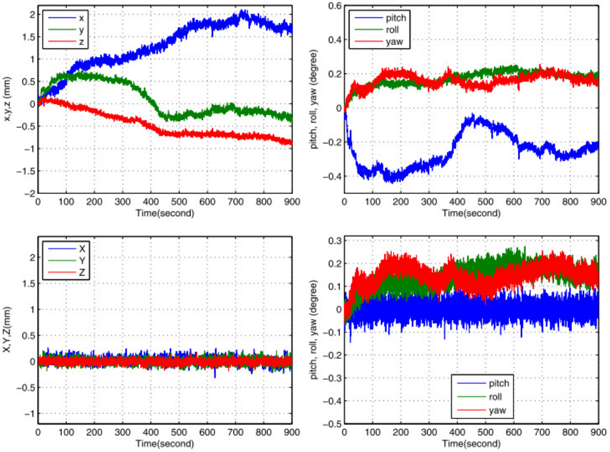

Time response of feedback control without (left) and with (right) decoupling control [Liu et al. (2015)].

Human Volunteer Feedback Motion Correction Results

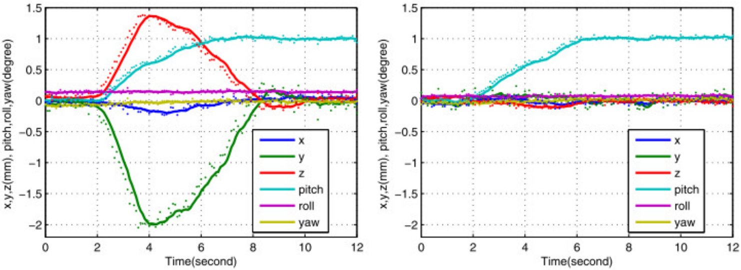

Head Motion Without and With Motion Correction. Left: Coupled Axes; Right: Decoupled Axes.

SRS: Wiersma Stewart-Gough Platform

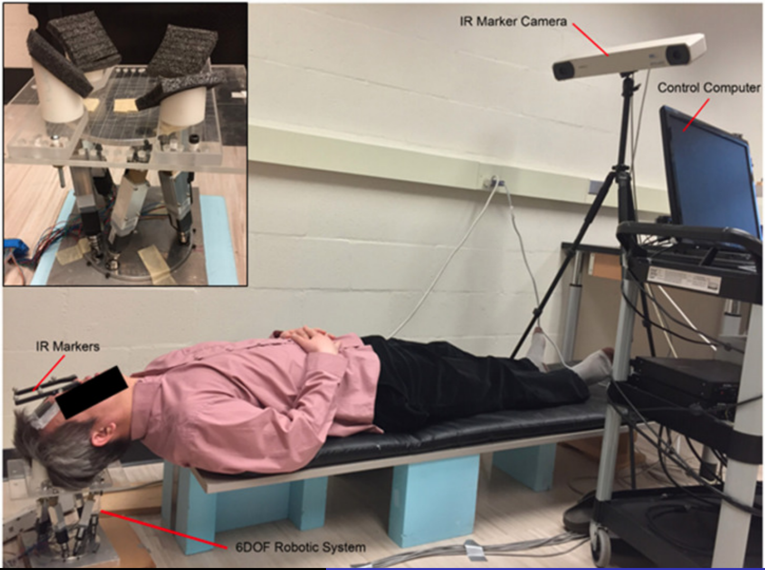

6-DOF Motion Correction Results

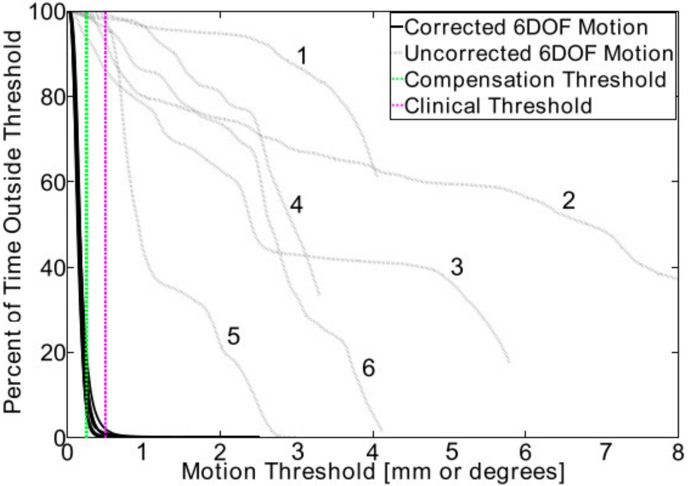

Next-Gen RT Treatment with MRI-LINACs

Elekta's Unity MRI-LINAC. Elekta

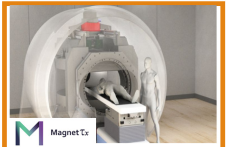

MRIDIAN by ViewRay: MR image guidance Radiation on table Adaptive Radiotherapy.

VIEWRAY®

MRI in LINAC RT

- Next generation precision beam delivery.
- High speed, high resolution MLC.
- Online plan adaptation capabilities.

- MRI that offers superior soft tissues visualization integrated with linear accelerator (LINAC) RT Offers unrivaled, online, and real-time cancer RT treatment [Raaymakers et al., Raaymakers et al.]
- Commercialized in systems such as
  - Elekta AB's (Sweden) 1.5T diagnostic imaging system [Raaymakers et al.];
  - Viewray 's MRIdian system [Mutic et al.]; or
  - the MagnetTx's (Canada) Aurora RT system [Fallone et al.] among others.
- Random and involuntary patient motion often occurs during image acquisition leading to
  - Artifacts ⇒ Poor image quality.
  - Incomplete irradiation of the tumor target.
  - Exposure of healthy tissues to radiation toxicity.
    - These lower the accuracy of online and real-time precise radiation dose delivery.
    - Affects clinical efficacy.

Pneumatic Actuated Soft Robots for Head Motion Compensation

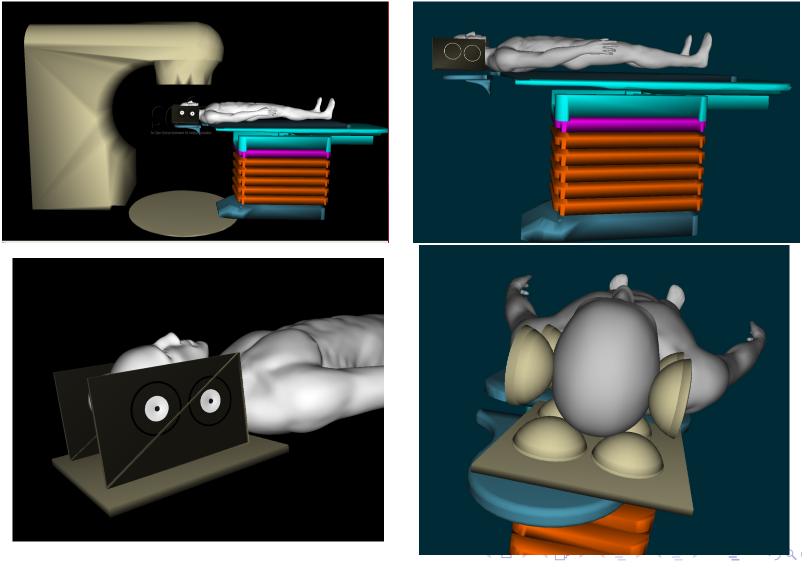

Cephalopods-inspired CCOARSE Actuator Design

Circumferentially Constrained And Radially Symmetric Elastomers [Pikul et al. (2019)].

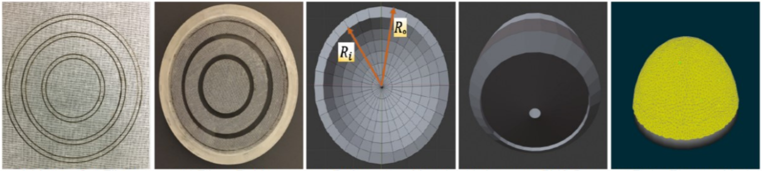

(a) Laser-Cut Fiber (b) Fiber+Rubber (c) Deformation Model (d) Actuator+PVC Base (e) Finite Element Model

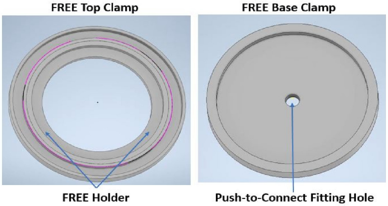

(f,g)

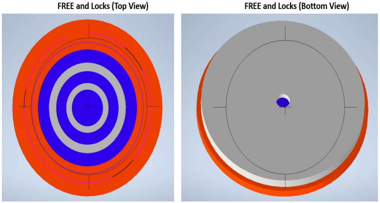

(h)

CCOARSE Actuator Schematic

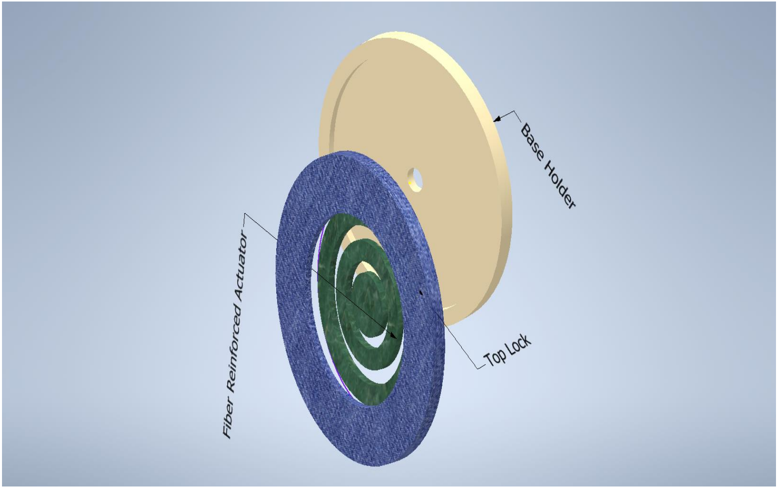

Nonlinear Elastic Deformation Analysis

IAB SHELLS AND AIR CAVITY/DEFORMATION ANALYSIS

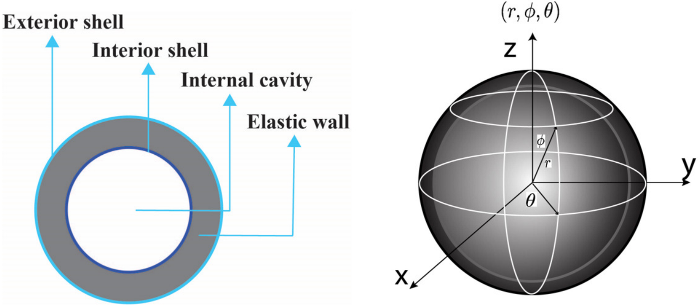

$$r_i \leq r \leq r_o, \qquad 0 \leq \theta \leq 2\pi, \qquad 0 \leq \phi \leq \pi$$

Soft IK via Boundary Value Problem

- Using the following boundary conditions for the Cauchy Stress,
  - $\sigma_{rr|R=R_0} = -P_{atm}, \sigma_{rr|R=R_i} = -P_{atm} - P$
- And together with Cauchy's first law, we find that
  - $\sigma_{rr}(r) = -\int_{r_i}^{r_o} [2C_1(\frac{r}{R^2} - \frac{R^4}{r^5}) + 2\,C_2\left(\frac{r^3}{R^4} - \frac{R^2}{r^3}\right)]dr$
  - $\sigma_{rr}(r) = \int_{R_i}^{R_o} [2C_1\left(\frac{1}{r} - \frac{R^6}{r^7}\right) - 2C_2\left(\frac{R^4}{r^5} - \frac{r}{R^2}\right)]\,dr$
- With $\sigma_{rr|R=R_i} = -P_{atm} - P$ and setting $P_{atm} = 0$, we find
  - $P(r) = \int_{r_i}^{r_o} [2C_1(\frac{r}{R^2} - \frac{R^4}{r^5}) + 2\,C_2\left(\frac{r^3}{R^4} - \frac{R^2}{r^3}\right)]dr$
  - $P(r) = \int_{R_i}^{R_o} [2C_1\left(\frac{1}{r} - \frac{R^6}{r^7}\right) - 2C_2\left(\frac{R^4}{r^5} - \frac{r}{R^2}\right)]\,dr$
  - $r^3 = R^3 + r_i^3 - R_i^3$ and $r_o^3 = R_0^3 + r_i^3 - R_i^3$

Volumetric Deformation Results (Simulation)

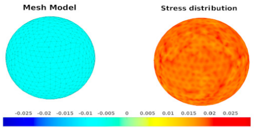

(a) **Left**: Mesh model. **Right**: Stress distribution on outer skin.

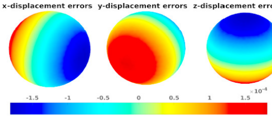

(b) Displacement errors along x, y, z coordinates.

Inputs					Outputs		
C_1	C_2	R_i	r_i	$R_\circ$	$r_\circ$	P	ΔV
$1.1e4$	$2.2e4$	$.027$	$.03$	$.03$	$.033$	$.76$	≈ 0

Fig. 6: Volumetric Deformation (Expansion).

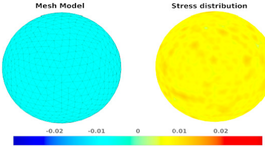

(a) **Left**: Mesh model. **Right**: Stress distribution on outer skin.

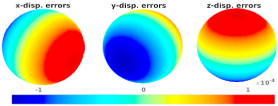

(b) Displacement errors along x, y, z coordinates.

Inputs					Outputs		
C_1	C_2	R_i	r_i	$R_\circ$	$r_\circ$	P	ΔV
$1.1e4$	$2.2e4$	$.025$	$.03$	$.03$	$.028$	$-.34$	≈ 0

Fig. 7: Volumetric Deformation (Compression).

Pneumatic Control and Deformation Scheme

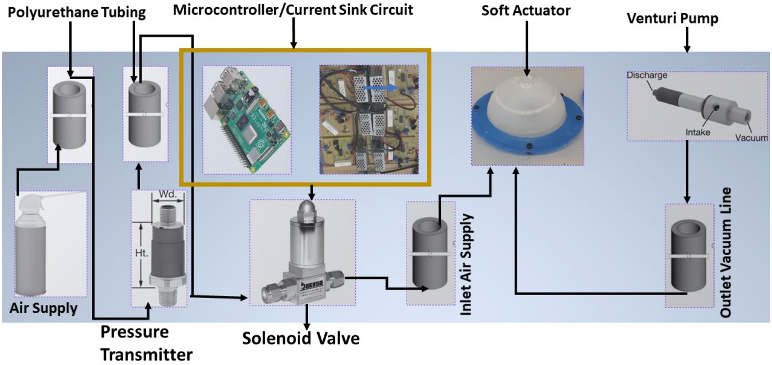

Volumetric Deformation Results (Actual)

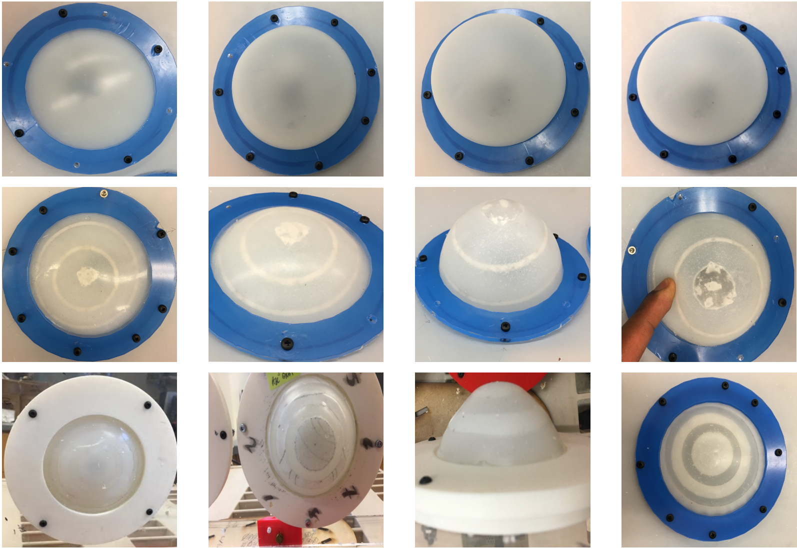

Head Motion Control (Independent Actuation)

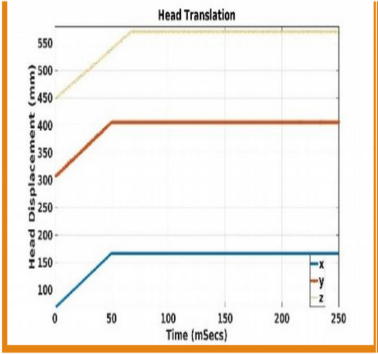

Head Translation along x, y, z for a task of raising the head by a certain threshold above the table

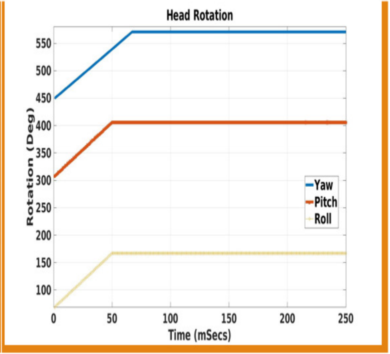

Head rotation in Euler angles for a task of tilting the head about the x, y, z axes on the treatment table.

Ongoing Work

Continuum Mechanical Model Validation/Differential Geometry/Newton-Euler Dynamics

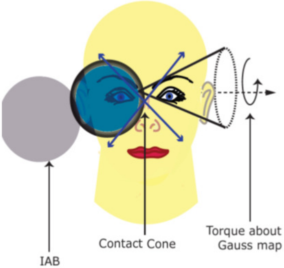

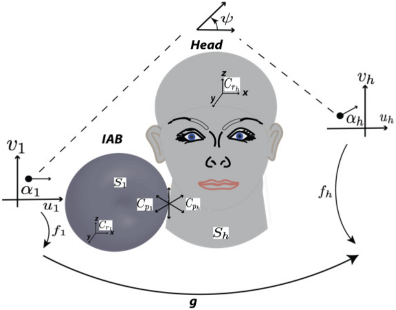

Part I.A: Beam Orientation Optimization (BOO)

- Beam Orientation Optimization (BOO)
  - Monte Carlo Tree Search and Neuro-Dynamic Programming for BOO

BOO Relevant Works

- Sadeghnejad Barkousaraie, Azar, **Olalekan Ogunmolu**, Steve Jiang, and Dan Nguyen. "A fast deep learning approach for beam orientation optimization for prostate cancer treated with intensity-modulated radiation therapy." In *Medical physics: International Journal of Medical Physics Research and Practice,* 47, no. 3 (2020): 880-897.
- **Ogunmolu, Olalekan**, Michael Folkerts, Dan Nguyen, Nicholas Gans, and Steve Jiang. "Deep BOO! Automating Beam Orientation Optimization in Radiation Therapy." In *Algorithm Foundations of Robotics XIII*, Merida, Mexico. Published in *Springer's Proceedings in Advanced Robotics (SPAR) Book*, 2020.
- Barkousaraie, Azar Sadeghnejad, **Olalekan Ogunmolu**, Steve Jiang, and Dan Nguyen. "Using Supervised Learning and Guided Monte Carlo Tree Search for Beam Orientation Optimization in Radiation Therapy." In *Workshop on Artificial Intelligence in Radiation Therapy*, pp. 1-9. Springer, Cham, 2019.
- Azar Sadeghnejad Barkousaraie, **Olalekan Ogunmolu**, Steve Jiang, and Dan Nguyen. "A Fast Deep Learning Approach for Beam Orientation Selection Using Supervised Learning with Column Generation on IMRT Prostate Cancer Patients." *Medical Physics (AAPM)* 46 (6), E237-E237, San Antonio, TX, July 2019.
- **Olalekan Ogunmolu**, Azar Sadeghnejad Barkousaraie, Nicholas Gans, Steve Jiang, and Dan Nguyen. "An Approximate Policy Iteration Scheme for Beam Orientation Selection in Radiation Therapy." *Medical Physics (AAPM)* 46 (6), E386-E386 San Antonio, TX, July 2019.
- Azar Sadeghnejad Barkousaraie, **Olalekan Ogunmolu**, Steve Jiang, and Dan Nguyen. "A Reinforcement Learning Application of Guided Monte Carlo Tree Search Algorithm for Beam Orientation Selection in Radiation Therapy." *Medical Physics (AAPM)* 46 (6), E236-E236, San Antonio, TX, July 2019.

Contributions

Relevant Publications

Ogunmolu, Olalekan, Michael Folkerts, Dan Nguyen, Nicholas Gans, and Steve Jiang. "Deep BOO! Automating Beam Orientation Optimization in Radiation Therapy." In *Algorithm Foundations of Robotics XIII*, Merida, Mexico. Published in *Springer's Proceedings in Advanced Robotics (SPAR) Book*, 2020.

- A sparse tree lookout strategy for games with large state spaces guides transition between beam angle sets
- Tree lookout strategy guided by a deep neural network policy

BOO Process: Fluence Map Optimization

Prostate CT slice

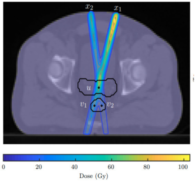

Prostate before BOO

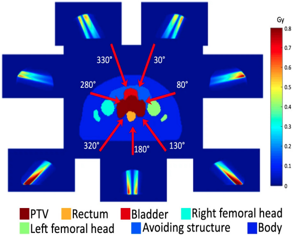

Fluence Map

Treatment Plan Flowchart

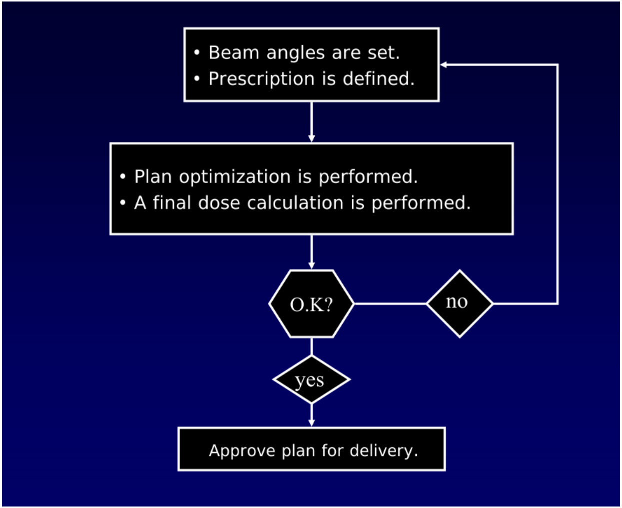

Reprinted from "IMRT Optimization Algorithms. David Shepard. Swedish Cancer Institute. AAPM 2007."

Current Approaches

- Stochastic optimization approaches: simulated annealing; genetic algorithms and gradient search, or a combination of genetic and gradient search algorithms.
- Mixed-integer programming, branch and cut/bound algorithms, beam angle elimination algorithms.
- Commercial planners use some highly non-convex objective (actual function is proprietary and unknown to public).

IMRT/BOO Motivation

- Beam orientations largely manually chosen or adopted from a standard protocol for clinical use.
- Pre-solve the dose influence matrices for each beam orientation.
- Then solve FMO.
- Time consuming (hours for dose fluence), and minutes for (FMO); Still solution is often not optimal.

Approach

- A Tower Neural Network generates a policy that guides MCTS simulations for two players in a zero-sum Markov game
  - Produces a *utility (value) function* & a subjective *probability distribution*
- Each player in a two-player Markov game finds an alternating best response to the current player's average strategy
  - driving the neural network policy's weights toward an approximate **saddle equilibrium** [Heinrich et al. (2015)].
  - aids network in finding an *approximately optimal* beam angle candidate set that meets a dosimetric requirements.

Data Preprocessing

- 77 anonymized patient CT scans, $\boldsymbol{D}$, and their dose influence matrices, $\mathcal{D}_{ij}$
- Scans shaped, $\boldsymbol{D} \times N \times H \times W$ from prostate cases in previous treatment plans
- Each slice resized to 64×64

State Representation: Prostate Organ Masks

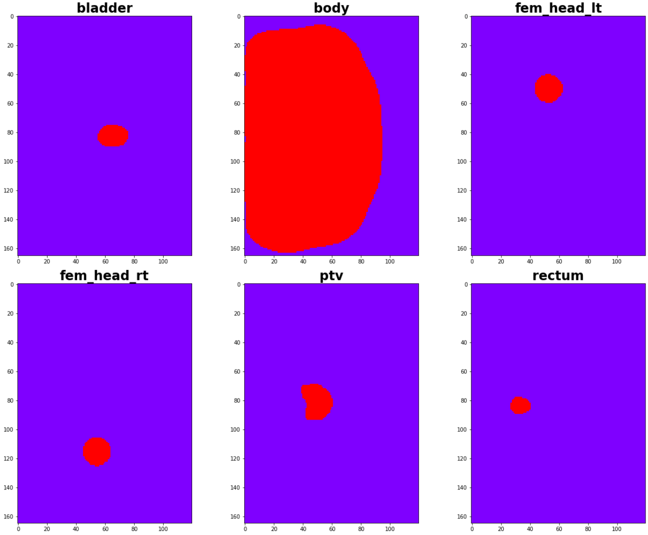

State Representation: Beam Angles

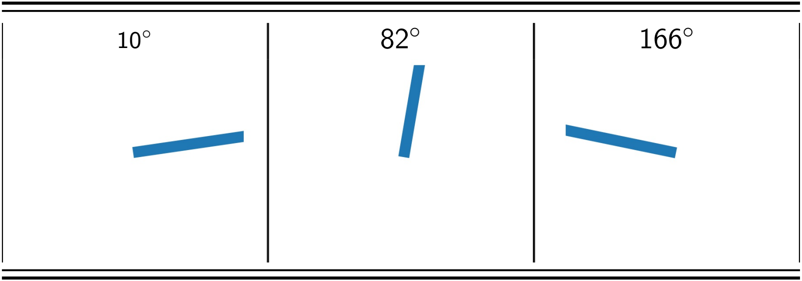

State Representation

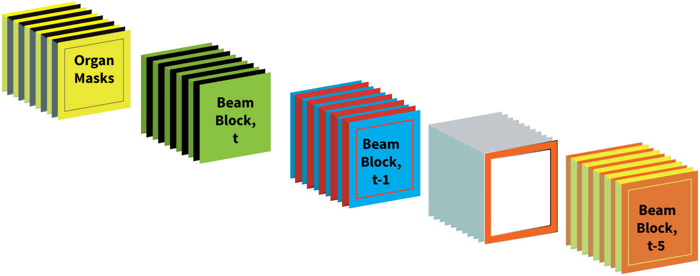

State Representation

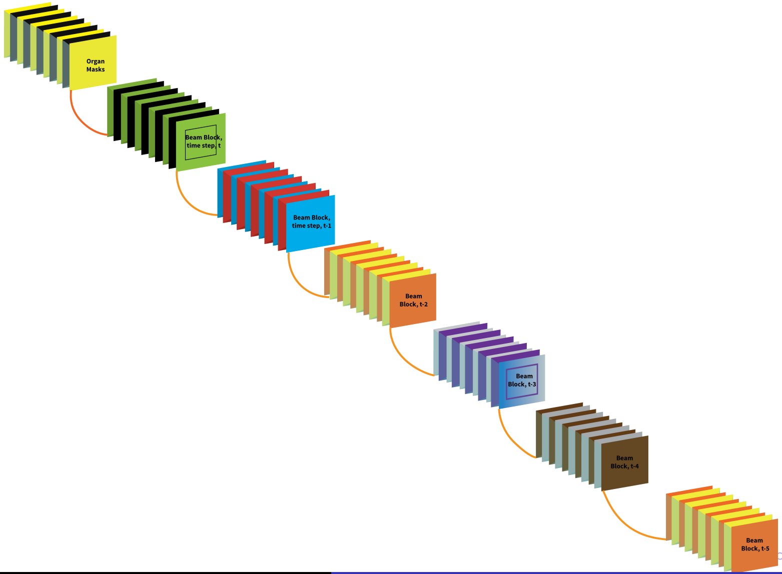

Tree Representation and Game Simulation

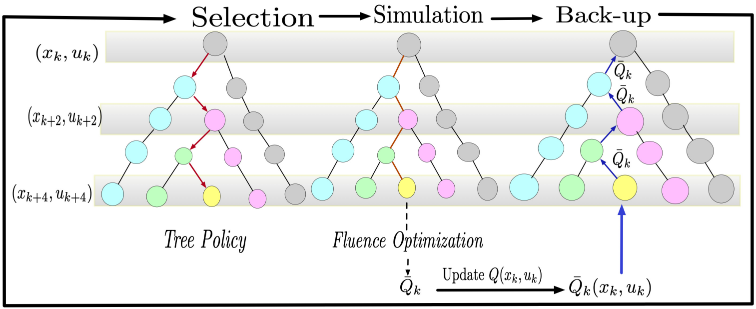

Tree Composition

Every **node** of the tree, $\boldsymbol{x}$, has the following fields:

- a pointer to the parent that led to it, $\boldsymbol{x}.p$;
- the beamlets, $\boldsymbol{x}_b$, stored at that node; $b = \{1, \ldots, m\}$;
- a set of move probabilities prior, $p(s, a)$;
- a pointer $\boldsymbol{x}.\boldsymbol{r}$, to the reward r_t, for the state $\boldsymbol{x}_t$;
- a pointer to the state-action value $Q(s, a)$ and its upper confidence bound $U(s, a)$;
- a visit count $N(s, a)$, that indicates the number of times that node was visited; and
- a pointer $\boldsymbol{x}.child_i$ to each of its children nodes.

Game Simulation: Mixed Strategies

- Each player, p_1, p_2, bases its decision on a random event's outcome
  - generating a **mixed strategy** determined by **averaging the outcome** of individual plays.
- Both players constitute a two-player **stochastic action selection strategy**: $\pi(s, a) = Pr(a|s) := \{\pi^{p_1}, \pi^{p_2}\}$ that gives the probability of selecting moves in any given state
- Suppose the game simulation starts from an initial condition s_0.

Saddle Point Strategy Formulation

- The **saddle point strategies** for an optimal control sequence pair $\{a_t^{p_1^*}, a_t^{p_2^*}\}$ can be recursively obtained by optimizing a state-action value cost, $\mathcal{J}_t(s, a)$

$$V_t^*(s) = Q_t^*(s_t, \pi_t^{p_1}, \pi_t^{p_2}) = \min_{\pi^{p_1} \in \Pi^{p_1}} \max_{\pi^{p_2} \in \Pi^{p_2}} Q_t^\star(s_t, \pi^{p_1}, \pi^{p_2})$$
$$\forall s_t \in \mathcal{S}, \pi^{p_1} \in \Pi^{p_1}, \pi^{p_2} \in \Pi^{p_2}.$$

such that

$$v_{p_1}^\star \leq v^\star \leq v_{p_2}^\star \quad \forall \{\pi_t^{p_1}, \pi_t^{p_2}\}_{0 \leq t \leq T}.$$

where $v_{p_i}^\star$ are the respective optimal values for each player.

Fluence Map Optimization

- $\mathcal{X} \implies$ total discretized voxels of interest (VOI's) in a target volume
- $\mathcal{B}_1 \cup \mathcal{B}_2 \cup \ldots \cup \mathcal{B}_n \subseteq \mathcal{B} \implies$ beam partition subset
- $\mathcal{D}_{ij}(\theta_k) \implies$ matrix that describes each dose influence, d_i
  - Computed by calculating each d_i for every bixel, j, at every φ°, resolution, where $j \in \mathcal{B}_k$

Methods: FMO problem definition

- Cost

$$\frac{1}{v_s} \sum_{s \in \text{OARs}} \|(b_s - \underline{w}_s \mathcal{D}_{ij}^s \boldsymbol{x}_s)_+\|_2^2 + \frac{1}{v_s} \sum_{s \in \text{PTVs}} \|(\bar{w}_s \mathcal{D}_{ij}^s \boldsymbol{x}_s - b_s)_+\|_2^2 \tag{1}$$

- Pre-calculated dose term: $\boldsymbol{Ax} = \{\sum_s \frac{w_s}{v_s} \mathcal{D}_{ij}^s \boldsymbol{x}_s \,|\, \mathcal{D}_{ij} \in \mathbb{R}^{n \times l}, n > l\}$

Methods: FMO

- Rewriting the objective

$$\min \frac{1}{2}\|A\mathbf{x} - \mathbf{b}\|_2^2 \quad \text{subject to } x \geq 0.$$

- With Lagrangian:

$$L(\boldsymbol{x}, \boldsymbol{\lambda}) = \min \frac{1}{2}\|A\mathbf{x} - \mathbf{b}\|_2^2 - \boldsymbol{\lambda}^T \boldsymbol{x}.$$

- Introducing an auxiliary variable $\mathbf{z}$, we have

$$\min_{\boldsymbol{x}} \frac{1}{2}\|\boldsymbol{A}\mathbf{x} - \mathbf{b}\|_2^2, \quad \text{subject to } \boldsymbol{z} = \boldsymbol{x}, \; \boldsymbol{z} \geq 0,$$

Methods: FMO by way of ADMM

- Solving either the $\boldsymbol{x}$ and $\boldsymbol{z}$ sub-problems, we have

$$\boldsymbol{x}^{k+1} = \left(\boldsymbol{A}^T\boldsymbol{A} + \rho \boldsymbol{I}\right)^{-1} \left(\boldsymbol{A}^T\boldsymbol{b} + \rho \boldsymbol{z}^k - \boldsymbol{\lambda}^k\right). \tag{2}$$

- And using the soft-thresholding operator, $S_{\boldsymbol{\lambda}/\rho}$, we find that

$$\boldsymbol{z}^{k+1} = S_{\boldsymbol{\lambda}/\rho}\left(\boldsymbol{x}^{k+1} + \boldsymbol{\lambda}^k\right), \tag{3}$$

where $S_{\boldsymbol{\lambda}/\rho}(\tau) = (x - \boldsymbol{\lambda}/\rho)_+ - (-\tau - \boldsymbol{\lambda}/\rho)_+$. $\boldsymbol{\lambda}$ is updated as

$$\boldsymbol{\lambda}^{k+1} = \boldsymbol{\lambda}^k - \gamma(\boldsymbol{z}^{k+1} - \boldsymbol{x}^{k+1}), \tag{4}$$

where γ is a parameter that controls the step length.

BOO Results: Testing of self-play network

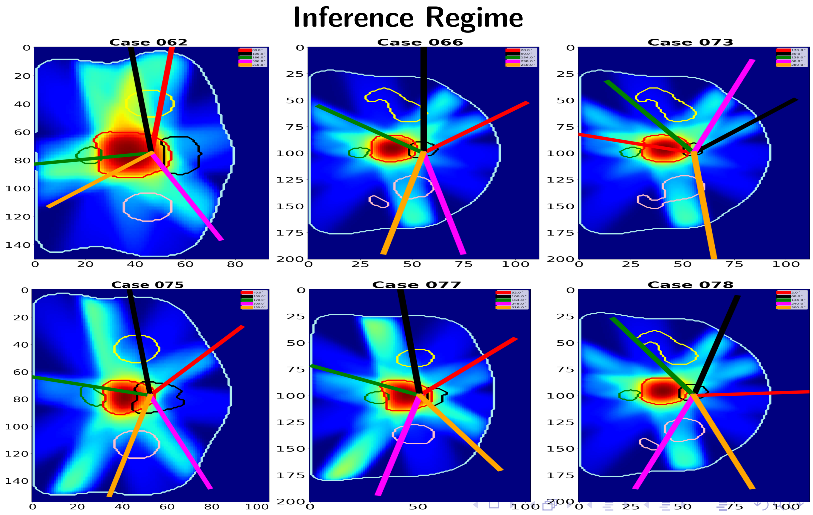

Part I.B: Supervised Column Generation Pretraining for BOO

- Beam Orientation Optimization (BOO)
  - Monte Carlo Tree Search and Neuro-Dynamic Programming for BOO
  - $\rightarrow$ Column Generation as Pretraining for Deep Neural Network BOO

Relevant Publication

- Sadeghnejad Barkousaraie, Azar, **Olalekan Ogunmolu**, Steve Jiang, and Dan Nguyen. "A fast deep learning approach for beam orientation optimization for prostate cancer treated with intensity-modulated radiation therapy." In *Medical physics: International Journal of Medical Physics Research and Practice,* 47, no. 3 (2020): 880-897.

Column Generation as Pretraining for DNN

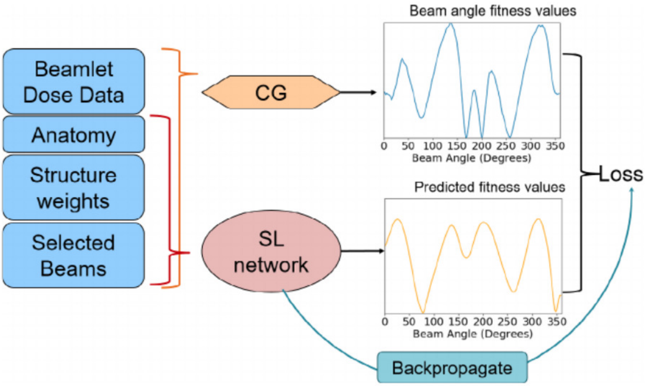

Network Structure

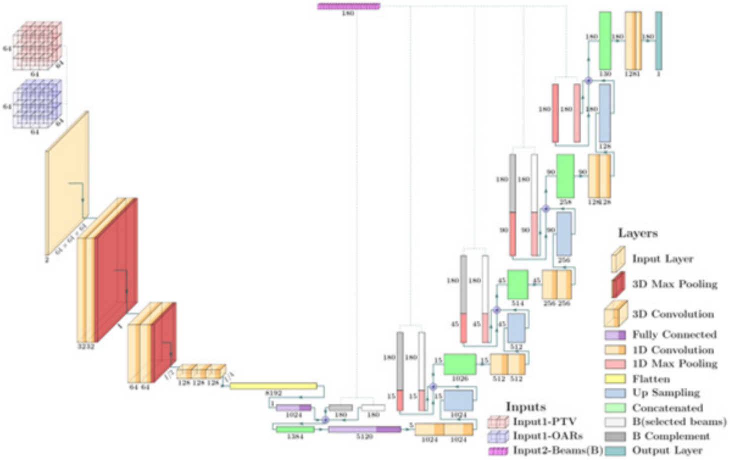

Training and Validation Loss

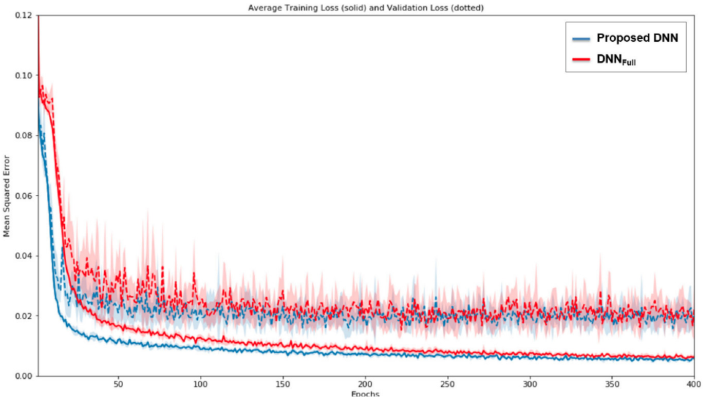

Average training (solid) and validation (dotted) loss function (MSE) values across six cross-validation folds for the network (blue) and full network.

Inference: Column Generation vs U-Net

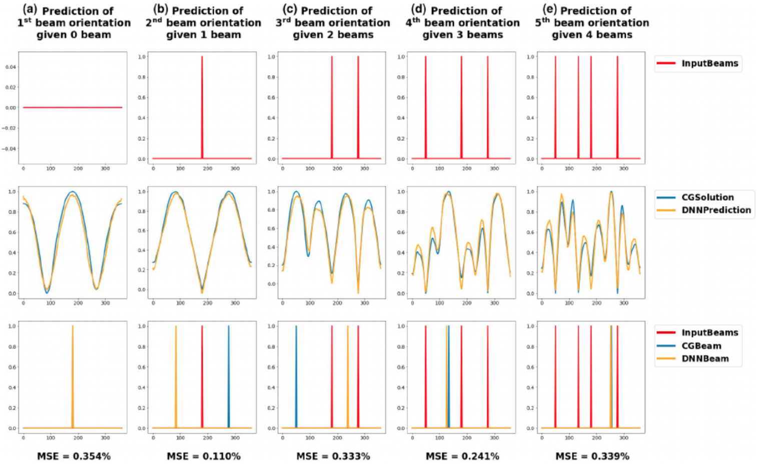

(a) Prediction of 1st beam orientation given no beam. (b) Prediction of 2nd beam orientation given 1 beam. (c) Prediction of 3rd beam orientation given 2 beams. (d) Prediction of 4th beam orientation given 3 beams. (e) Prediction of 5th beam orientation given 4 beams.

Dose Washes of Column Generation vs Neural Network

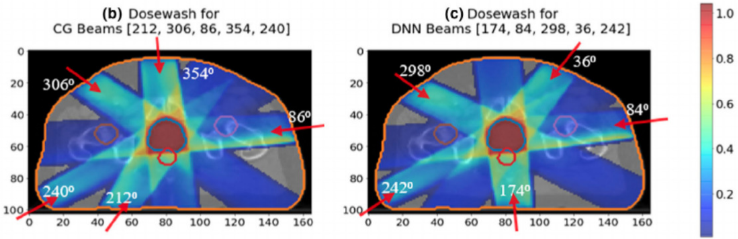

Dose-Volume Histogram of CG vs DNN architectures

Dose Volume Histograms

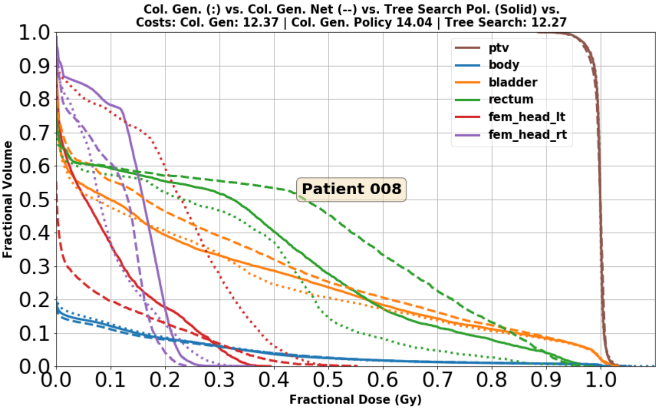

Conclusions

- Finding the good beam angle candidates is orders of magnitude faster than the current approaches
  - Based on a neural network generative model of an MDP
  - Sparse lookahead search builds tree with nodes labeled by state-action pairs in an alternating manner (2-3 minutes).
  - Tree built stagewise from root to nodes has fixed depth; sample rewards stored on edges connecting state-action with state nodes
- Beam angles prediction takes between 2-3 minutes with MCTS vs 1 minute with Column Generation Pretraining.

Part III: Robustness Margins and Robust Deep Policies

- Robustness Margins and Robust Deep Policies for Nonlinear Control

Iterative Dynamic Game

Relevant Papers

- Ogunmolu, Olalekan, Nicholas Gans, and Tyler Summers. "Minimax iterative dynamic game: Application to nonlinear robot control tasks." In 2018 *IEEE/RSJ International Conference on Intelligent Robots and Systems (IROS)*, pp. 6919-6925. IEEE, 2018.
- Ogunmolu, Olalekan, Nicholas Gans, and Tyler Summers. "Robust zero-sum deep reinforcement learning." *arXiv preprint arXiv:1710.00491* (2017).
- Summers, Tyler, Olalekan Ogunmolu, Nicholas Gans. "Robustness Margins and Robust Guided Policy Search for Deep Reinforcement Learning." In *IEEE/RSJ International Conference on Robots and Intelligent Systems,(Abstract Only Track)*, vol. 8. 2017.

The robustness conundrum

- How to know *a priori* a policy's robustness limits?

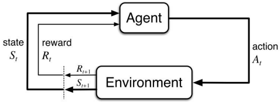

- How to inculcate robustness into multistage decision policies?

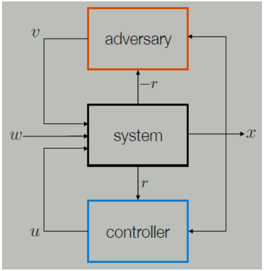

Problem Setup

- To quantify the brittleness, we optimize the stage cost

$$\max_{\mathbf{v}_t \sim \psi \in \Psi} \left[\sum_{t=0}^{T} \underbrace{c(\mathbf{x}_t, \mathbf{u}_t)}_{\text{nominal}} - \gamma \underbrace{g(\mathbf{v}_t)}_{\text{adversarial}} \right]$$

- To mitigate lack of robustness, we optimize the *cost-to-go*

$$\mathcal{J}_t(\mathbf{x}_t, \pi, \psi) = \min_{\mathbf{u}_t \sim \boldsymbol{\pi}} \max_{\mathbf{v}_t \sim \psi} \left(\sum_{t=0}^{T-1} \ell_t(\mathbf{x}_t, \mathbf{u}_t, \mathbf{v}_t) + L_T(\mathbf{x}_T) \right),$$

- and seek a saddle point equilibrium policy that satisfies

$$\mathcal{J}_t(\mathbf{x}_t, \pi^*, \psi) \le \mathcal{J}_t(\mathbf{x}_t, \pi^*, \psi^*) \le \mathcal{J}_t(\mathbf{x}_t, \pi, \psi^*),$$

Results: Brittleness Quantification

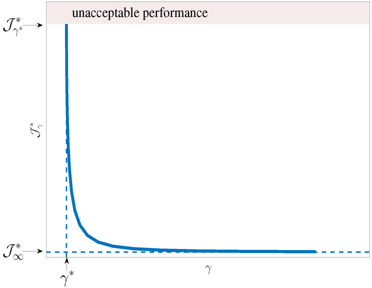

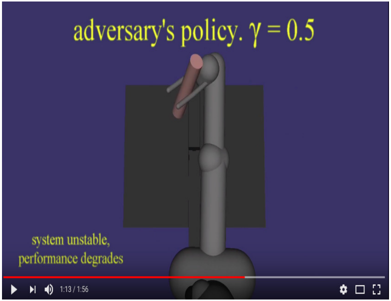

Results: Iterative Dynamic Game

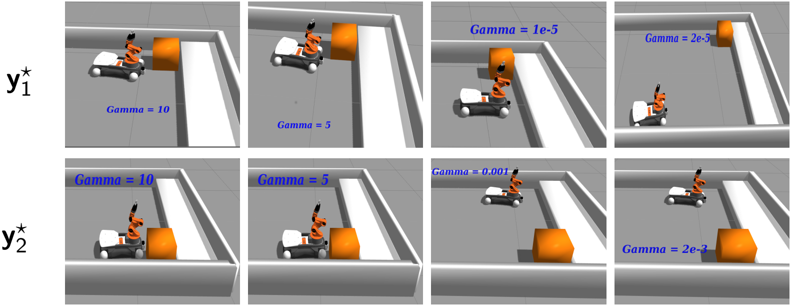

End pose of the KUKA platform with our iDG formulation given different goal states and γ-values

Future Work: MRI/RT Immobilization

- Explore multiple parallel robot mechanisms for head motion correction.
- Adopt iterative dynamic game approach [Ogunmolu et al. (2018)] for solving robust controller for head stabilization.
- Build on Freeman and Kokotovic's point-wise min-norm robust control lyapunov function to realize a meaningful value function in deep policies [Freeman and Kokotovic (1996)].

Publications

- **Ogunmolu, Olalekan**, Xinmin Liu, Nicholas Gans, and Rodney D. Wiersma. "Mechanism and Model of a Soft Robot for Head Stabilization in Cancer Radiation Therapy." In *2020 IEEE International Conference on Robotics and Automation (ICRA)*, pp. 4609-4615. IEEE, 2020.
- **Ogunmolu, Olalekan**, and Rodney D. Wiersma. "Kinematics and Kinects of a Continuum Parallel Soft Robot for MRI-LINAC Motion Correction." Working Paper, In *IEEE Transactions on Robotics*, IEEE 2020.
- **Ogunmolu, Olalekan** and Rodney D. Wiersma. "A Real-Time Patient Head Motion Correction Mechanism for MRI-Linac Systems." In *2020 Virtual Joint AAPM|COMP Meeting*,AAPM 2020.
- **Ogunmolu, Olalekan**, Xinmin Liu, Rodney D. Wiersma. "Auto-Determination of the Dextrous WorkSpace in Robotic Stereotactic Radiosurgery." In *2020 Virtual Joint AAPM|COMP Meeting*, AAPM 2020.

Publications

- **Ogunmolu, Olalekan**, Gans, Nicholas, Jiang, Steve, and Gu, Xuejun. "SU-E-J-12: An Image-Guided Soft Robotic Patient Positioning System for Maskless Head-And-Neck Cancer Radiotherapy: A Proof-Of-Concept Study." *Medical Physics* 42, no. 6Part7 (2015): 3266-3266.
- **Ogunmolu, Olalekan P.**, Xuejun Gu, Steve Jiang, and Nicholas R. Gans. "A real-time, soft robotic patient positioning system for maskless head-and-neck cancer radiotherapy: an initial investigation." In *2015 IEEE International Conference on Automation Science and Engineering (CASE)*, pp. 1539-1545. IEEE, 2015.
- **Ogunmolu, Olalekan P.**, Xuejun Gu, Steve Jiang, and Nicholas R. Gans. "Vision-based control of a soft robot for maskless head and neck cancer radiotherapy," In *2016 IEEE International Conference on Automation Science and Engineering (CASE)*, pp. 180-187.IEEE, 2016.
- **Ogunmolu, Olalekan**, Adwait Kulkarni, Yonas Tadesse, Xuejun Gu, Steve Jiang, and Nicholas Gans. "Soft-neuroadapt: A 3-dof neuro-adaptive patient pose correction system for frameless and maskless cancer radiotherapy." In *2017 IEEE/RSJ International Conference on Intelligent Robots and Systems (IROS)*, pp. 3661-3668. IEEE, 2017.
- Almubarak, Yara, Joshi, Aniket, **Ogunmolu, Olalekan**, Gu, Xuejun, Jiang, Steve, Gans, Nicholas, and Tadesse, Yonas. "Design and development of soft robot for head and neck cancer radiotherapy." In *Electroactive Polymer Actuators and Devices (EAPAD)* XX, vol. 10594, p. 1059418. International Society for Optics and Photonics, 2018.

End of Slides

Thank you!

Radhini Chelvarajah, Brigid Leighton, Linda Martin, Wayne Smith, and Rachael Beldham-Collins. Cranial immobilisation—is there a better way? *Radiographer*, 51(1):29–33, 2004.

Xinmin Liu, Andrew H Belcher, Zachary Grelewicz, and Rodney D Wiersma. Robotic stage for head motion correction in stereotactic radiosurgery. In *2015 American Control Conference (ACC)*, pages 5776–5781. IEEE, 2015.

Andrew Belcher. *Patient Motion Management with 6-DOF Robotics for Frameless and Maskless Stereotactic Radiosurgery*. PhD thesis, The University of Chicago, 2017.

Olalekan Ogunmolu and Rodney Wiersma. A Real-Time Patient Head Motion Correction Mechanism for MRI-Linac Systems. In *Joint AAPM | COMP Meeting, Virtual*, 2020.

James Pikul, Itai Cohen, and Robert Shepherd. Stretchable surfaces with programmable texture, May 2 2019. US Patent App. 16/161,029.

PC Parks. Liapunov Redesign of Model Reference Adaptive Control Systems. *IEEE Transactions on Automatic Control*, 11(3):362–367, 1966.

Olalekan Ogunmolu, Adwait Kulkarni, Yonas Tadesse, Xuejun Gu, Steve Jiang, and Nicholas Gans. Soft-NeuroAdapt: A 3-DOF Neuro-Adaptive Patient Pose Correction System for Frameless and Maskless Cancer Radiotherapy. In *IEEE/RSJ International Conference on Intelligent Robots and Systems (IROS), Vancouver, BC, CA*, pages 3661–3668. IEEE, 2017.

Johannes Heinrich, Marc Lanctot, and David Silver. Fictitious self-play in extensive-form games. In *International Conference on Machine Learning*, pages 805–813, 2015.

Olalekan Ogunmolu, Nicholas Gans, and Tyler Summers. Minimax Iterative Dynamic Game : Application to Nonlinear Robot Control. *IEEE International Conference on Intelligent Robots and Systems*, 2018.

Randy A Freeman and Petar V Kokotovic. Inverse optimality in robust stabilization. *SIAM journal on control and optimization*, 34(4):1365–1391, 1996.